Neutron Stars: Investigating their Mass-Radius Relationship

Sophia Baker (Supervisor: Dr Nigel Metcalfe)
Submitted: 24-03-2020

We find mass-radius relationships for two different neutron star composition models, using a polytropic equation of state $P = K\epsilon^{\gamma}$ and solving the hydrostatic equilibrium (HE) equations in both their non-relativistic and relativistic forms. Assuming a pure neutron composition, the non-relativistic HE equations yield an infeasible maximum mass, 5.19 $M_{\odot}$, highlighting the importance of relativistic corrections. The relativistic Tolman-Oppenheimer-Volkov (TOV) correction gives a maximum mass of 1.02 $M_{\odot}$ and a 6th degree polynomial relationship. Below the maximum, mass increases as radius decreases. There is a discrepancy of $\sim$55% between our computed masses and those measured observationally for in the 10.0 - 11.5 km radius range. The inclusion of an iron-56 crust has significant adverse effects, with the masses found using the TOV model more comparable to the mass of Earth than to that of a star. No fit is applied due to the random oscillatory nature of the relationship. We discuss our results in context of observational and literature values, along with reasons for the iron crust model's failure, sources of uncertainty, and potential improvements to both models (namely the inclusion of repulsive nucleon-nucleon interactions).

I Introduction

I.1 Neutron Stars: A Summary

Type Ib, Ic and II supernovae are the spectacular finale to the life of main sequence stars with mass greater than 8 $M_{\odot}$. The outer layers of the stars are ejected in a highly energetic explosion, leaving behind a dense core of degenerate matter. This remnant is a neutron star. Classes of neutron star include pulsars, magnetars and x-ray binary systems.

Though termed "stars", neutron stars are no longer active nuclear fusion sites. As such, gravitational collapse has no opposition via thermal pressure. Equilibrium must instead be reached via other forces.

Typically, a neutron star has a radius $r \approx 10$ km and a mass in the range $1.4M_{\odot} \leq M \leq 2.5M_{\odot}$. In other words, the average density of a neutron star, ρ, is similar to that of an atomic nucleus ($\rho \approx 10^{17}$ kgm^{-3}). At such high densities, matter becomes degenerate - the neutrons, which are fermions, are so tightly packed that they are forced to occupy high states of kinetic energy so as not to violate the Pauli Exclusion Principle [1]. This is the source of neutron degeneracy pressure, which offers support against gravitational collapse for masses up to 0.7 $M_{\odot}$ [2]. However, we know from observational data that neutron star can be more massive than this. Nucleon-nucleon interactions are the missing piece, allowing for masses up to 2.16 $M_{\odot}$ [3].

Neutron stars are composed of predominantly of neutrons. There is, however, variation in composition with changing radius, i.e. changing density and pressure, as shown in figure 1. At the stellar surface, pressure is sufficiently low to sustain a crystalline outer "crust" of free electrons and atomic nuclei such as iron-56. This nuclei-rich layer spans densities up to 3×10^{17} kgm^{-3}. By approximately 4×10^{14} kgm^{-3}, however, it is no longer the most energetically favourable option for neutrons to remain bound in the nuclei and they free themselves, "dripping" out of the nuclei. The region in which this process occurs is known as the neutron drip layer [5].

As density increases, the number of neutrons relative to nuclei increases further until in the outer core, over 90% of matter present is neutrons, the rest being protons and electrons. The outer core is typically a superfluid liquid.

Neutrons begin to overlap geometrically when ρ reaches

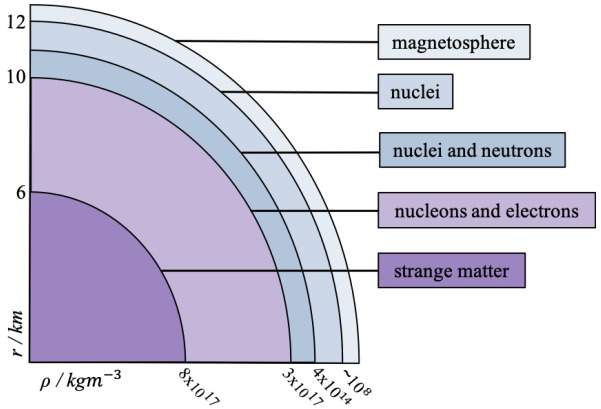

Figure 1: Diagram to show the composition of a 1.5 $M_{\odot}$ neutron star [4]. Pressures are low enough at the stellar surface to host atomic nuclei, whereas at the core, pressures are so high they give rise to strange states of matter such as hyperons or Bose-Einstein condensates of mesons or kaons [3].

4 times the atomic saturation density. In the inner core of the neutron star, ρ exceeds atomic saturation density by a factor of 5-10. It is hence theorised to play host to strange states of matter such as hyperons (strange hadrons containing no charm, top or bottom quarks [6]) or Bose-Einstein condensates of mesons or kaons [4][3].

I.2 Modelling Internal Structure

The internal structure of a star is modelled with the hydrostatic equilibrium equations:

$$\frac{dP}{dr} = -\frac{GM(<r)\rho(r)}{r^2} \tag{1}$$

and

$$\frac{dM}{dr} = 4\pi r^2 \rho(r), \tag{2}$$

where P is pressure, r is radius, $M(<r)$ is enclosed mass, ρ is mass density and G is the gravitational constant [1].

However, a neutron star is made up of relativistic degenerate matter and so we must apply relativistic corrections to (1) in the form of the Tolman-Oppenheimer-Volkov equation [2]:

$$\frac{dP}{dr} = -\frac{GM(<r)\epsilon(r)}{c^2 r^2}\left[1+\frac{P(r)}{\epsilon(r)}\right] \left[1+\frac{4\pi r^3 P(r)}{M(<r)c^2}\right]\left[1-\frac{2GM(<r)}{c^2 r}\right]^{-1}, \tag{3}$$

given here in terms of the energy density, ϵ:

$$\epsilon = \rho c^2, \tag{4}$$

where c is the speed of light in a vacuum. All constants and their errors as defined by NIST (see appendix).

The central pressure of a neutron star is most simply given by a polytropic equation of state (EoS) in the form:

$$P = K\epsilon^{\gamma}. \tag{5}$$

Relativistic and non-relativistic matter are described by different K and γ. Ignoring nucleon-nucleon interactions, and assuming pure neutron composition, for non-relativistic neutron star matter, $\gamma^n_{nr} = \frac{5}{3}$, and K_{nr} is given by:

$$K^n_{nr} = \frac{\hbar^2}{15\pi^2 m_n}\left(\frac{3\pi^2 Z}{A m_n c^2}\right)^{\frac{5}{3}}, \tag{6}$$

where $\hbar$ is the reduced Planck constant, m_n is neutron mass, and $\frac{A}{Z}$ is the atomic mass ratio; in this case $\frac{A}{Z} = 1$. We calculate its numerical value to be $K^n_{nr} = (2.9836 \pm 0.0007)\times 10^{25}\ \mathrm{kg}^{-\frac{2}{3}}\mathrm{m}^2$.

For relativistic neutron star matter under the same assumptions, $\gamma^n_r = 1$, and K_r simplifies to:

$$K^n_r = \frac{1}{3}. \tag{7}$$

We use the relativistic model when particles' energy exceed their rest mass energy (when the condition $k_F c >> m_n c$ is satisfied) and non-relativistic otherwise.

These models account only for support against gravitational collapse via neutron degeneracy pressure [1].

I.3 Finding the Mass-Radius Relationship

There are thought to be around 100 million neutron stars in the Milky Way [7]. However, of these, we only know the masses of around 35 [3], and although observational data can suggest ranges within which their radii may lie, until very recently it was not possible to obtain an accurate value of radius. Even so, this can only be done under very specific conditions; the recent high precision radius measurement of a $M = 1.4\ \mathrm{M}_\odot$ neutron star was achieved via the combination measurements of the gravitational waves produced by the neutron star merger GW170817 and electromagnetic observations of the neutron star remnant of this collision [11]. Merger events are not necessarily a typical neutron star formation mechanism, so this a limited use technique. The challenging nature of accurate radius measurements is one reason why the development of good models for the mass-radius relationship is so crucial.

This, and and modelling the internal structure of neutron stars, is also important as we are unable to replicate the high pressures and consequent exotic matter found in neutron star cores in a laboratory setting [3].

In this work, we trial various models of internal structure to determine the neutron star mass-radius relationship and compute the neutron star mass limit, i.e. the minimum mass of a black hole, for each model, and the radius at which it occurs. For quick reference we label each combination of assumptions and models (see table 1).

Label	HE	Composition
1a	Non-Relativistic	Pure Neutron
1b	TOV (Relativistic)	Pure Neutron
2a	Non-Relativistic	Iron Crust
2b	TOV (Relativistic)	Iron Crust

Table 1: Labels assigned to each combination of assumptions and models and their resulting mass-radius relationships. Hydrostatic equilibrium equations is abbreviated to "HE."

We find the mass-radius relationship by simultaneous solving the HE equations, in whichever form called upon by the model in question. This is a process we have carried out via integration "by hand," a method chosen to account for the radius-dependent density term $\rho(r)$. The $\rho - r$ relationship is not explicitly defined, so ρ must be numerically determined and substituted into our calculations at each step of integration. The integration "by hand" method also allows for the switch between relativistic and non-relativistic polytropes as required at different radii, and for the changes in composition presented in models 2a and 2b.

For a given neutron star of known central pressure P_C, we first choose our initial conditions to be $r \approx 0$, $M \approx 0$ and $P = P_C$. It is important to note that r and M cannot be exactly equal to 0, as this would result in a divide-by-zero error in the calculations that follow.

We define our neutron star such that the surface pressure $P_S = 0$. The total radius and mass are hence the r and M corresponding to this P, i.e. we repeat the above integration steps until the condition $P = P_S$ is met.

For changing composition models, the first step is to determine composition based on current ρ. We assume a pure neutron composition, and so use the polytropic equations of state with constants as defined in equations (6) and (7), unless $\rho \geq 10^{14}$, the density at which neutrons start to "drip" from iron-56 and other nuclei, for which we adapt equation (6) to:

$$K^{Fe}_{nr} = \frac{\hbar^2}{15\pi^2 m_e}\left(\frac{3\pi^2 Z}{A m_n c^2}\right)^{\frac{5}{3}}, \tag{8}$$

where $\frac{A}{Z} = 2.25$ and m_e is the mass of an electron. This is because the dominant form of degeneracy pressure in this nucleus/free-electron region is electron degeneracy pressure rather than its neutron counterpart; we model the iron crust as a Fermi gas of electrons.
Next we calculate the Fermi momentum in order to determine the appropriate equation of state:

$$k_F = \hbar\left(\frac{3\pi^2\rho}{m_n}\frac{Z}{A}\right)^{\frac{1}{3}}, \tag{9}$$

with variables and constants as defined previously. This is calculated the same for pure neutrons and for the iron-56 crust, for which we assume the neutron mass dominates over electron mass.

If $k_F c > m_n c$, choose the relativistic polytrope; otherwise, choose the non-relativistic polytrope [1].

We now "step out" by Δr, so let $r = r_{previous} + \Delta r$, and calculate the pressure at this new radius, $P = P_{previous} + \Delta P$. ΔP is calculated by rearranging $\frac{dP}{dr} = \frac{\Delta P}{\Delta r}$. This is necessary (a) to check the condition for integration $P > 0$ is satisfied, and (b) to allow calculation of ρ for this step in r, the next step in the process. Rearranging the chosen equation of state, and substituting in the current P, yields the current ρ:

$$\rho = \left(\frac{P}{K}\right)^{\frac{1}{\gamma}} \frac{1}{c^2}. \tag{10}$$

We can hence calculate M by rearranging $\frac{dM}{dr} = \frac{\Delta M}{\Delta r}$ and substituting in the current r and ρ. Each time we calculate a new value, we also calculate its uncertainty using methods described in [8].

Once these steps are complete, if $P < 0$, the current r and M are taken to be the neutron star's total mass and radius. Otherwise, the steps are repeated. The process is shown in figure 2.

It is important to recognise that if Δr is too large, we may overshoot the true maximum radius. A balance must be struck between step size and computation time. In this work we use $\Delta r = 1 \times 10^{-5}$ km.

This process is repeated over a range of central pressures to give the mass-radius relationship for a range of neutron stars. The range of central pressures are chosen such that central density exceeds the average density of a neutron star.

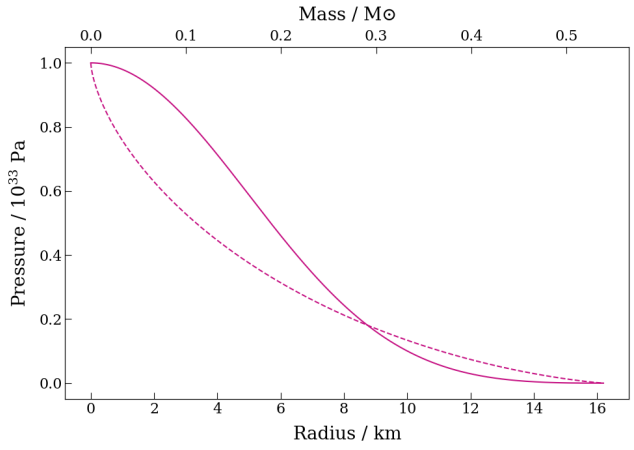

Figure 2: Plot to show the pressure-radius (solid line) and pressure-mass (dashed line) relationships for a neutron star with $P_C = 1 \times 10^{33}$ Pa. Pressure decreases with increasing radius, and therefore with enclosed mass, until it dips below zero at the neutron star's maximum radius. This "dip" is not large enough to be visible on this plot. Note that in this plot mass and radius refer to a radius within a neutron star, and the mass enclosed in that radius, not the total masses and radii of multiple neutron stars.

II Results

II.1 1a and 1b: Pure Neutron / NDP Models

We find a mass-radius relationship under the assumption that gravitational collapse is prevented solely via neutron degeneracy pressure. This simplification, which we will refer to as the NDP model, is applied to pure neutron and iron-56 crust neutron star for the TOV and non-relativistic HE equations. The relationships obtained are plotted in figures 3 and 4.

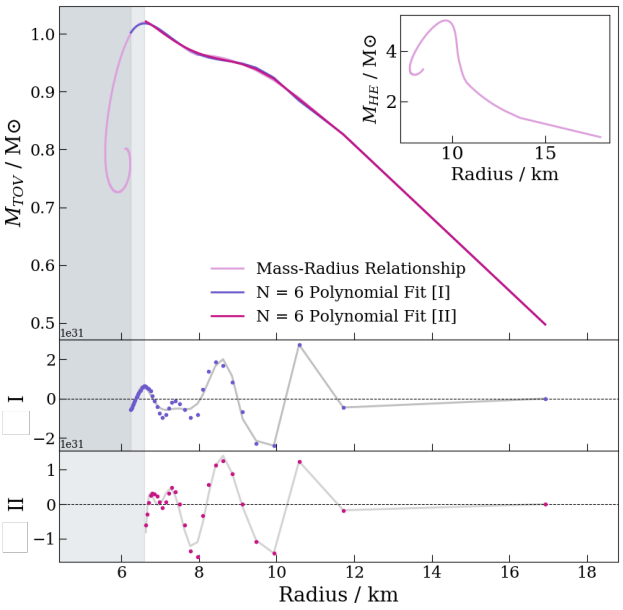

Figure 3: Plot to show the mass-radius relationship as determined from models 1a and 1b, with the main plot showing 1b, and the inset 1a. As the non-relativistic HE relationship yields a non-feasible maximum mass, we have not applied a fit. The TOV relationship, however, is fitted with a 6th degree polynomial for two regions. Fit I extends to beyond M_{max}, to include points in the unstable region, whereas fit II is only applied to the stable region, including points up to M_{max}. Here we refer to stability against radial oscillations. Normalised residuals are plotted for the TOV relationship and these fits (labelled I and II); there is high-order polynomial structure present, as demonstrated by the grey line, which is a simple 20th degree polynomial fit. This suggests that our chosen model would benefit from the inclusion of some higher order terms. We have not fitted the region where multiple r give the same M. Computed errors on M are all negligibly small. We take error on r to be $\Delta r = 1 \times 10^{-5}$ km. Neither set of error bars has been plotted, scaled or otherwise, to avoid overcrowding.

The pure neutron model yields a maximum mass M_{max} = 5.19 $M_\odot$ at r = (9.66801 $\pm$ 0.00001) km from the non-relativistic HE equations and M_{max} = 1.02 $M_\odot$ at r = (6.59601 $\pm$ 0.00001) km from the TOV model. We have not quoted errors on M_{max} as they are of the order of 10^{-34}, a negligible proportion of the total value. For this model, up to the maximum mass, the higher the central pressure, the lower the radius and higher the mass.

The 6th degree polynomial fits seen in figure 3 are given by:

$$M = ar^6 + br^5 + cr^4 + dr^3 + er^2 + fr + g \tag{11}$$

with a, b, c, d, e, f and g as defined in table 2 for each version of the fit.

Despite appearing to be good fits by inspection, with the differences between calculated masses and those given by the fits only being of the order of 10^{-3} $M_\odot$, the normalised residuals and χ^2 for each fit suggest the opposite. We find that $\chi^2_{\nu_I} = 9.89 \times 10^{61}$ and $\chi^2_{\nu_{II}} = 6.94 \times 10^{61}$, implying an incredibly poor fit. These high χ^2_ν values are the result of vastly underestimated errors.

Errors are calculated via combination of error in r and errors in constants used using methods detailed in [8]. The error in r is our dominant error, being a factor of 10^6 greater than

Constants	Fit I	Fit II
a / $M_\odot$ km^{-6}	-1.42×10^{-4}	-8.01×10^{-5}
b / $M_\odot$ km^{-5}	0.00875	0.00492
c / $M_\odot$ km^{-4}	-0.220	-0.122
d / $M_\odot$ km^{-3}	2.88	1.60
e / $M_\odot$ km^{-2}	-20.8	-11.4
f / $M_\odot$ km^{-1}	78.7	42.5
g / $M_\odot$	-121	-63.7

Table 2: Constants from equation (11). Fits I and II are as defined in figure 3.

the next largest error. However, we have not considered the reduction in precision caused by computational errors e.g. floating point errors.

The non-relativistic model has not been fitted with an equation due to the infeasible nature of the maximum mass. The Schwarzschild radius, r_S, is the minimum physical radius that a spherically symmetric object of mass M can have before it collapses and becomes a black hole [4]:

$$r_S = \frac{2GM}{c^2}. \tag{12}$$

For an object with M = 5.19 $M_\odot$ the Schwarzschild radius is 15.3 km. This is a factor of 1.58 greater than the radius given by our model. The implication of this is that a M = 5.19 $M_\odot$, r = (9.7 $\pm$ 0.1) km object cannot be a neutron star, and would instead be a black hole. This is further supported by observational data; the stellar black hole in system GRO J0422+32, claimed to be the smallest observed black hole in the galaxy, has M = 3.97 $\pm$ 0.95 $M_\odot$ [9], with more recent research suggesting that this number may be much lower [10]. The maximum mass of a neutron star should be less that the minimum mass of a black hole.

The literature Tolman-Oppenheimer limit of 0.7 $M_\odot$ is 31% lower than maximum mass yielded by model 1b. One explanation for this is that we have not considered rounding errors or floating point errors, both of which are likely due to the nature of the computational methods used.

Ideally, we would now plot and fit the true neutron star mass-radius relationship for comparison with each model, but given the lack of measured neutron star radii, this is not possible. We can, however, compare the results corresponding to the recent mass-radius data obtained for merger GW170817, as mentioned in section I.3. The radius of the merger's remnant is the highest precision neutron star radius measurement to date at r = 11.0$^{+0.9}_{-0.6}$ km. Using our polynomial models, we calculate $M_1 1.0km$ at this radius, comparing the results to the true mass as observed at this radius, 1.4 $M_\odot$ [11]. For models I and II:

$$M^I_{11.0\text{km}} = (0.85^{-0.02}_{+0.04})\ M_\odot \tag{13}$$

and

$$M^I_{11.0\text{km}} I = (0.86^{-0.04}_{+0.04})\ M_\odot \tag{14}$$

respectively, both around 61% of their true counterpart.

We carry out a similar calculation using some other less precise neutron star mass-radius data. The radii of three pulsars of known mass in the 1.9 $M_\odot$ to 2.0 $M_\odot$ range have been measured to lie between 10.0 km and 11.5 km. Substitution of these radius constraints into our model yields:

$$M^I_{10.0\text{km}} = 0.920\ M_\odot, \tag{15}$$

$$M^I_{11.5\text{km}} = 0.829\ M_\odot, \tag{16}$$

$$M^{II}_{10.0\text{km}} = 0.919\ M_\odot \tag{17}$$

and

$$M^{II}_{11.5\text{km}} = 0.833\ M_\odot \tag{18}$$

All of these masses fall below the true mass range for these given radii, sharing a 54% ($M_{10.0\text{km}}$) and 56% ($M_{11.5\text{km}}$) percentage difference with their true counterparts. The discrepancy between M_{max} and the mass limit 2.16 $M_\odot$ is similar (53%).

(Note that it is obvious from figure 3 that we will not obtain a sufficiently high mass from these radii, but we calculate the expected masses for our models nonetheless to allow for quantitative comparison.)

II.2 2a and 2b: Iron Crust / NDP Models

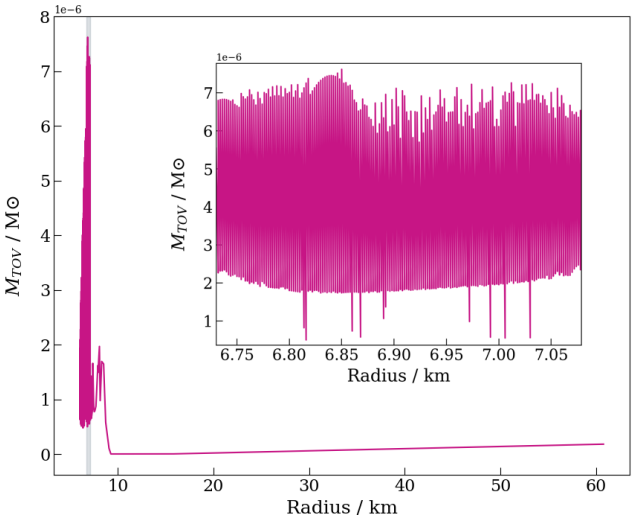

Figure 4: Plot to show the mass-radius relationship as determined from model 2b. Model 2a is excluded for clarity, as are error bars (which for M are only of the order 10^{-77} $M_\odot$ to 10^{-74} $M_\odot$). The mass-radius relationship oscillates so violently at low radii that no good fit can be applied; see the inset, which corresponds to the narrow grey shaded region.

The iron-56 crust model was applied for the same range of initial pressures as models 1a and 1b. As is evident from figure 4, it yields very different results.

Model 2a yields M_{max} = (1.79×10^{-43}) $M_\odot$ at r = (17.92601 $\pm$ 0.00001) km. The TOV model, 2b, gives M_{max} = (7.62×10^{-6}) $M_\odot$ at r = (6.11001 $\pm$ 0.00001) km. Though this radius is similar to that given by 1b, and 2a's radius is of a similar order of magnitude to 1a's, M_{max} is much too low for both 2a and 2b. Even the more massive of the two is more comparable to the mass of the Earth than to that of a star.

A higher P_C does not necessarily result in a higher r in this model. We re-order the values produced with respect to r, as opposed to with respect to P_C as in models 1a an 1b, to produce a more coherent plot.

We find the masses for the same radii as considered for the pure neutron model; all are of the order of 10^{-7} $M_\odot$.

There are obviously some major limitations to the iron crust model. One is that in a real life neutron star, there is not an absolute cut-off where composition changes from crystalline nuclei to neutron superfluid and the main source of supportive pressure changes from electron to neutron degeneracy pressure, as is assumed in this work. Though iron-56 nuclei can still be sustained up to densities 3×10^{17} kgm^3, free neutrons may be present when the pressure is 3 orders of magnitude smaller than this (as described in section I.1, neutrons gradually 'drip' out beyond a certain critical pressure). This is not accounted for in these iron-56 crust models [5].

II.3 Evaluation of Numerical Methods

It is possible to verify that the numerical methods used in this work are sound by quickly applying them to find the mass-radius relationship of a white dwarf star and comparing this to the known white dwarf mass-radius relationship.

A main sequence star of mass less than 8 $M_\odot$ will evolve to form a white dwarf star, typically composed of ionised carbon and oxygen nuclei. Electron degeneracy pressure is the last source of pressure supporting the star against gravitational collapse [4]. Like neutron degeneracy pressure, electron degeneracy pressure can only prevent collapse up to a finite mass limit,1.44 $M_\odot$, the Chandrasekhar mass limit [12].

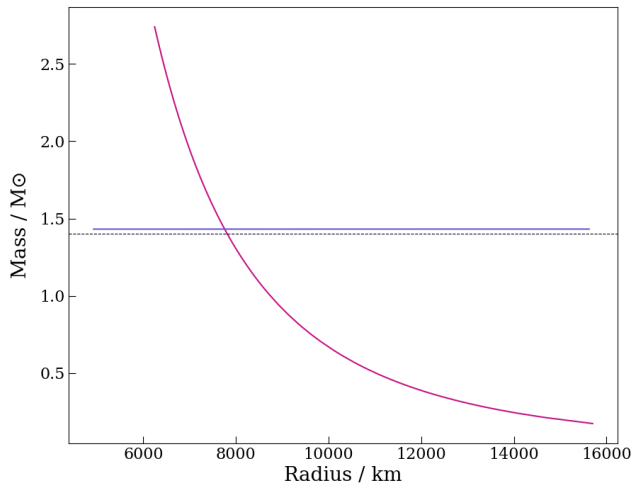

Figure 5: The mass-radius relationship of a white dwarf star for the assumptions that (a) the whole star is made up of non-relativistic matter (pink) and that it is made only of relativistic matter (purple). The dashed black line represents the Chandrasekhar mass limit.

We assume a pure carbon-12 white dwarf ($\frac{A}{Z}$ = 2.00) and from the Fermi gas model obtain:

$$K_{nr}^{WD} = \frac{\hbar^2}{15\pi^2 m_e}\left(\frac{3\pi^2 Z}{A m_n c^2}\right)^{\frac{5}{3}}, \tag{19}$$

for non-relativistic regions of the star, and

$$K_{r}^{WD} = \frac{\hbar^2}{12\pi^2}\left(\frac{3\pi^2 Z}{A m_n c^2}\right)^{\frac{4}{3}}, \tag{20}$$

for relativistic regions. The condition for relativity remains $k_F c >> m_n c$, with k_F as defined in equation (9). The numerical values of these constants are calculated to be K_{nr}^{WD} = (1.7279 $\pm$ 0.0003)$\times10^{-22}$ kg$^{-\frac{2}{3}}$m^2 and K_{r}^{WD} = (1.211771276365 $\pm$ 0.00000000000002)$\times10^{-13}$. White dwarf density is low enough that we need only solve the non-relativistic hydrostatic equilibrium equations.

In the non-relativistic regime, the mass-radius relationship takes the form:

$$M \propto R^{-3}. \tag{21}$$

Our model corresponds well to this observed mass-radius relationship and maximum mass, as is shown by the gradient of the log$R$-log$M$ relationship, and our relativistic model's asymptote at M = 1.43 $M_\odot$, only 2% different to the Chandrasekhar mass limit (see figure 5). These results bring us confidence in the validity of our method for determining the neutron star mass-radius relationship, and suggest that the numerical methods employed are not to blame for discrepancies from observed mass-radius data in our neutron star mass-radius relationship.

III Opportunities for Further Expansion

The models examined in this work are very simple, and are missing some crucial factors which could potentially enable us to reproduce observational data with our calculated values. The factor with the largest impact is the inclusion nucleon-nucleon interactions. Repulsion between nucleons in a neutron star provides a great deal of support against gravitational collapse and so would increase the mass limit calculated. A new expression for energy density involving nucleon-nucleon potential energy would be required (also including asymmetrical proton-neutron potential), leading to a new set of polytropes.

With the exception of the iron crust, we have assumed pure neutron composition throughout this work. This is despite the knowledge that neutron stars also contain protons, electrons, nucleon-nucleon pairs, and potentially exotic matter at high densities.

We have assumed that the number of protons and electrons is insignificant as many will be short-lived, being used up in the production of more neutrons via electron capture:

$$^1_1p + {}^0_{-1}e \longrightarrow {}^1_0n \tag{22}$$

However, some protons and electrons are still present in a neutron star. In the $\rho = 8\times10^{16}$ kgm^{-3} to 8×10^{17} kgm^{-3} region, neutron-neutron and proton-proton pairs are theorised to form. These pairs have integer spin i.e they are bosons, and they behave like a superfluid. There are sufficiently few of these pairs (only formed from 10% of nucleons) that they do not affect the equation of state, which is why they have not been considered. In neutron star formation, vast amounts of mass are lost. As momentum must be conserved, this leaves the neutron star itself rotating very rapidly, with rotational frequencies of up to 716 Hz recorded [13]. We approximate neutron stars as spheres, when in fact their rotation means that they are more accurately described as oblate spheroids. Whether or not this and other rotational effects make a difference to the amount of mass a neutron star can support depends on the frequency of the rotation. The models investigated in this work do not take into account rotational motion, as at moderate speeds, rotational corrections are only

of the order of a few percent [3]. However, it is suggested elsewhere that a rigidly spinning neutron star can support a maximum mass 15 - 20% higher than that of a stationary neutron star (corresponding to a radius increase of 30 - 40%) [14]. Whether or not rotational effects make a significant impact on mass and radius is therefore something worth investigating, and not just in terms of the maximum mass and range of masses supported, but also of the mass-radius relationship itself.

There comes a point between the nuclei crust and liquid outer core at which the nuclear and coulomb interactions of protons and neutrons are balanced and competing for dominance; the resultant nucleon complex theorised to form is known as 'nuclear pasta'. Such matter includes the gnocchi, lasagna and spaghetti phases at different densities, named due to the pasta-like appearance of their structures. This layer is thought to lie beyond the neutron drip layer but before the superfluid neutron liquid, and to only be around 0.1 km thick [15].

Something our models do not tell us is minimum neutron star mass. The minimum stable mass of a neutron star is thought to be M_{min} = 0.1 $M_\odot$ [16], which is lower than the lowest mass accounted for in models 1a and 1b. A possible extension to this work would be to cover a larger range of neutron stars, i.e. increase the range of central pressures used to include some lower values, and investigate the mass-radius relationship up to and beyond where we expect a minimum - is there a clear change in polarity of gradient, or does our polynomial model not apply to all values, allowing for infinitely low mass neutron stars?

IV Conclusions

When considering a neutron star composed solely of neutrons, we find that the mass-radius relationship, when we neglect relativistic effects, yields an infeasible mass limit. We hence conclude that relativistic corrections to the hydrostatic equilibrium equations are vital in modelling the mass-radius relationship of neutron stars. A mass limit of 1.02 $M_\odot$ is computed when considering relativistic effects. The neglect of nucleon-nucleon interactions means that this value falls well below many observed neutron star masses; for neutron stars in the 10.0 - 11.5 km radius range, masses given by this model fall short of measured masses in this range by approximately 55%. Our maximum mass has similar discrepancy with the literature mass limit, 2.16 $M_\odot$. Despite this, we fit an equation to the relationship, finding a 6th degree polynomial to be the most appropriate. Structure in the normalised residuals implies the need for higher order terms; however, the errors used to calculate these are vastly underestimated.

The inclusion of an iron crust presents us with no clear mass-radius relationship and as such no fit is applied. Although the model presents us with some plausible radii, the masses given are orders of magnitude too low, with the relativistic TOV correction yielding maximum mass of (3.85×10^{-47}) $M_\odot$. The model's failure may be due to its extreme simplicity; we have assumed a pure iron layer, supported by electron degeneracy pressure, which immediately gives way to pure neutrons once an exact pressure condition is met. This is not how a neutron star is structured, and free neutrons are gradually introduced over a pressure gradient. We conclude that this approach to modelling changing neutron star composition is not valid, and that the relativistic pure neutron model is the most preferable of the models we have investigated.

References

[1] B.W. Carrol & D.A. Ostlie, "An Introduction to Modern Astrophysics," 2nd Edition, Pearson, UK (2007)

[2] J.R. Oppenheimer & G.M. Volkov, Phys. Rev., **55** (1939)

[3] F. Özel & P. Freire, Annu. Rev. Astron. Astrophys., **54** (2016)

[4] R.L. Bowers & T. Deeming, "Astrophysics I: Stars," Jones and Bartlett, USA (1984)

[5] M. Coleman Miller, "Introduction to neutron stars," `http://www.astro.umd.edu/~miller/nstar.html` (accessed 25-02-20)

[6] W. Greiner, Lecture Notes in Physics, **581** (2001)

[7] M. Camenzind, "Compact Objects in Astrophysics: White Dwarfs, Neutron Stars and Black Holes," Springer, Germany (2007)

[8] I.G. Hughes & T.P.A. Hase, "Measurements and their Uncertainties," Oxford University Press, UK (2010)

[9] D.M. Gelino & T.E. Harrison, ApJ, **599** 2 (2003)

[10] L. Kreidberg et al., ApJ, **757** 36 (2012)

[11] C.D. Capano et al., Nat. Astron., **4** 3 (2020)

[12] S. Chandrasekhar, ApJ, **74** 81 (1931)

[13] J.W. Hessels et al., Science, **311** (2006)

[14] I.A. Morrison, T.W. Baumgarte & S.L. Shapiro, ApJ, **610** (2004)

[15] J.P. Lastota et al., ApJ, **456** (1996)

[16] L. Kaper et al., ESO Messenger, **126** (2006)

[17] E. Tiesinga et al., "Values of Fundamental Physical Constants," `https://physics.nist.gov/cuu/Constants/index.html` (accessed 10-03-20)

V Appendix

V.1 Constants and their Uncertainties

x	Constant	Uncertainty
G	6.67430×10^{-11}	0.00015×10^{-11}
c	$2.99\ 792\ 458\times10^{8}$	N/A
$\hbar$	$(6.626\ 070\ 15\times10^{-34})/2\pi$	N/A
m_n	$1.674\ 927\ 498\ 04\times10^{-27}$	$0.000\ 15\times10^{-27}$
m_e	$9.109\ 383\ 7015\times10^{-31}$	$0.000\ 000\ 028\times10^{-31}$

Table 3: Constants used in this work, listed in order of appearance. Their respective uncertainties, denoted as α_x, are as used in the calculation of combined uncertainties e.g. $\alpha_{K_{nr}}$, α_M. All values are from NIST [17].

In this work, the majority of sources of error are from the constants used to calculate our values of K and $\frac{dP}{dr}$, from which other values and their errors stem. These constants and their uncertainties are defined in table 3.

V.2 Units of Calculated Constants

We find the units of K_{nr} by dimensional analysis, e.g.:

$$[K_{nr}^n] = \frac{[\hbar]^2}{[m_n]} \left(\frac{1}{[m_n][c]^2} \right)^{\frac{5}{3}} = \frac{J^2 s^s}{kg} \left(\frac{1}{kgm^2 s^{-2}} \right)^{\frac{5}{3}}. \quad (23)$$

With the substitution J = kg $m^2 s^{-2}$, we get $[K_{nr}]$ = $kg^2 m^4 s^{-4} s^4 kg^{-\frac{8}{3}} m^{-2}$ = $kg^{-\frac{2}{3}} m^2$. K_r is confirmed to be dimensionless similarly.